UAV Deployment and IoT Device Association for Energy-Efficient Data-Gathering in Fixed-Wing Multi-UAV Networks

Yung-Ching Kuo, *Graduate Student Member, IEEE*, Jen-Hao Chiu, Jang-Ping Sheu, *Fellow, IEEE*, and Y.-W. Peter Hong, *Senior Member, IEEE*

***Abstract*—This work studies the deployment of multiple fixed-wing unmanned aerial vehicles (UAVs) for data-gathering from ground IoT devices and the corresponding device association policy. Each UAV is assumed to follow a circular flight trajectory above its responsible network area in order to stay afloat. The device association and the UAVs' trajectory centers and radii are jointly optimized to maximize the total energy savings of the devices. Given the trajectory centers and radii, the device association problem is modeled as a multiple 0-1 knapsack problem, and solved by a two-stage maximum energy-saving (MES) device association policy. Moreover, given the device association, the UAVs' trajectory centers and radii are optimized by an iterative load-balancing (ILB) algorithm, where the trajectory centers are chosen as a load-dependent weighted sum of their associated devices' locations. Furthermore, we also propose a collision-free scheduling policy that minimizes the total phase offset between the actual and ideal transmission phases of all devices, and a modified MES algorithm that provides higher association priority to devices whose data gathered by the UAV is more outdated. Simulation results show that the proposed MES and ILB algorithms outperform candidate schemes in terms of the total energy savings of IoT devices.**

***Index Terms*—UAV communications, Internet of Things, energy saving, resource allocation, wireless coverage, device association, UAV placement, scheduling.**

I. Introduction

THE USE of unmanned aerial vehicles (UAVs) as flying wireless communication platforms has received much attention in recent years due to the UAVs high mobility and deployment flexibility [1], [2]. In cellular applications, UAVs have been adopted as temporary base stations (BSs) to provide rapid service recovery in case of natural disasters [3] and also for data offloading during special events or hot spots [4]. UAVs can also serve as mobile relays or form flying ad hoc networks to provide coverage extension or connectivity between distant or separated users [5]–[7]. In Internet-of-Things (IoT) or wireless sensor networks (WSNs), UAVs have also been used as mobile aggregators to enable efficient data gathering from ground sensor devices [8], [9]. In this case, the UAVs' 3D placement or trajectory design as well as the power control and association decisions of IoT devices must be carefully designed in order to fully exploit these advantages. Two types of UAVs have been considered the most in the literature, namely, rotary-wing and fixed-wing UAVs. Rotary-wing UAVs can hover above fixed positions and, thus, allow more flexible trajectory designs, but are less energy-efficient. Fixed-wing UAVs, on the other hand, have larger payload, higher speed, and longer lifetime, but must maintain constant movement in order to stay afloat. While the former provides flexible on-demand usage of UAVs for emergency applications, we argue that the latter is more suitable for long-term surveillance or environmental monitoring applications. In this work, we are interested in the use of multiple fixed-wing UAVs for efficient data-gathering in IoT and WSNs.

Specifically, the use of UAVs for data collection in IoT has been examined in the literature for cases with single [10], [11] and multiple UAVs [12]–[15], respectively. In [10], the UAV's trajectory and the sensors' wake-up schedule were jointly determined to minimize the maximum energy consumption of all sensors while ensuring that a target amount of data from each sensor is collected reliably by the UAV. In [11], the UAV's trajectory was designed to minimize the flight time while allowing each sensor to upload a certain amount of data with limited energy consumption. Moreover, in [12], a joint design of multiple rotary-wing UAVs' 3D placement, device association, and uplink power control was determined by minimizing the transmission power of ground devices subject to constraints on the signal-to-interference-plus-noise ratio (SINR) at the UAVs. In [13], the UAVs' placement was determined by maximizing the average number of bits that are transmitted by the ground users under constraints on the maximum hover time of UAVs. The authors leveraged results from optimal transport theory to determine the optimal partitioning of the geographical area, taking into consideration the UAVs' hover times and locations. In [14], the UAV deployment, device association, and uplink resource allocation were jointly optimized for multiple rotary-wing UAVs with the goal of maximizing the lifetime of ground devices. Moreover, [15] considered the 3D placement of multiple UAVs in a three-tier space-air-ground heterogeneous

Manuscript received February 13, 2021; revised May 28, 2021; accepted June 21, 2021. Date of publication June 29, 2021; date of current version November 22, 2021. This work was supported in part by the Ministry of Science and Technology, Taiwan, under Grant MOST 109-2634-F-007-015, Grant 109-2221-E-007-079-MY3, and Grant 110-2634-F-007-021. This work was presented in part at Globecom 2020. *(Corresponding author: Y.-W. Peter Hong.)*

Yung-Ching Kuo, Jen-Hao Chiu, and Jang-Ping Sheu are with the Department of Computer Science, National Tsing Hua University, Hsinchu 30013, Taiwan (e-mail: cludbuster@gmail.com; q910553@gmail.com; sheujp@cs.nthu.edu.tw).

Y.-W. Peter Hong is with the Institute of Communications Engineering and MOST Joint Research Center for AI Technology and All Vista Healthcare, National Tsing Hua University, Taipei 10617, Taiwan (e-mail: ywhong@ee.nthu.edu.tw).

Digital Object Identifier 10.1109/TGCN.2021.3093453

2473-2400 © 2021 IEEE. Personal use is permitted, but republication/redistribution requires IEEE permission.
See https://www.ieee.org/publications/rights/index.html for more information.

Authorized licensed use limited to: National Tsing Hua Univ.. Downloaded on March 09,2022 at 07:46:55 UTC from IEEE Xplore. Restrictions apply.

network. A two-stage joint hovering altitude and power control problem was solved by taking into consideration the cross-tier interference. Different from [12]–[15], our work considers the deployment of multiple fixed-wing UAVs, and the association of IoT devices to maximize the total uplink energy savings of the devices. We assume that each UAV follows a periodic circular flight trajectory above its associated devices in order to stay afloat. This is also different from several other works, e.g., [16], [17], that focus on trajectory designs that dynamically adapt to real-time changes in the environment, including sensor activation, channel conditions, and quality-of-service demands etc. We argue that, by following a simple circular trajectory, the design complexity and computational overhead can be significantly reduced, and the deployment can be more robust to uncertainties in the environment. In this case, the UAVs' trajectory centers and radii must be carefully chosen so that most devices are located along the trajectories rather than close to the center of the circle. Hence, the simple K-means solution often used in the placement of rotary-wing UAVs is not suitable for our problem.

In this work, we examine a joint UAV deployment and IoT device association problem that aims to maximize the total energy savings of devices during the data-gathering process by multiple UAVs. The total energy savings is defined as the sum of the energy savings experienced by IoT devices that have been successfully associated with the UAVs (and, thus, are allowed to transmit). This objective measures the impact of the UAVs' locations on both the minimum required transmission power of the devices and their association decisions. An efficient solution is obtained by solving successively the UAV deployment and the IoT device association subproblems under the ideal scheduling scenario. Then, practical considerations on the transmission scheduling and user fairness are further examined. In particular, a collision-free scheduling policy is proposed to avoid interference among devices associated with the same UAV, and a maximum weighted energy-saving problem is proposed to ensure fairness among devices. It is worthwhile to note that, while this work focuses on the uplink transmission from the devices to the UAVs, the data collected by the circulating UAVs can be further sent to a central data-gathering node using, e.g., multi-hop transmissions, as examined in [18]. In particular, the main contributions of this paper can be summarized as follows:

- First, given the UAVs' trajectory centers and radii, the IoT device association subproblem is modeled as a 0-1 multiple knapsack problem with assign restrictions (MKPAR) [19], [20], which is known to be NP-hard. We propose a two-stage maximum energy-saving (MES) device association policy, where each UAV first solves a single knapsack problem locally by considering all connectable devices, and then resolves conflict with other UAVs using a maximum profit assignment scheme.
- Moreover, given the device association, the UAVs' trajectory centers and radii are optimized using an iterative load-balancing (ILB) algorithm, where the centers are chosen as a load-dependent weighted sum of its associated devices' locations. The algorithm takes into consideration both the load of the devices as well as the relative distance between the devices and their closest point on the circular trajectory of the UAVs.
- To avoid interference among closely located devices, whose transmission durations are likely to overlap, we further propose a collision-free scheduling policy based on the minimization of the total phase offset between the ideal and actual transmission phases of all the devices.
- Also, to address the issue of fairness, we propose a data-freshness-aware device association policy that gives higher priority to devices whose data gathered by the UAV is more outdated.
- Extensive simulation results are provided to demonstrate the effectiveness of the proposed MES and ILB algorithms compared to the conventional equal-probability association and K-means deployment. The collision-free scheduling and data-freshness-aware association are also shown to effectively reduce the loss due to collision avoidance and enhance fairness.

The remainder of this paper is organized as follows. Section II introduces related works on UAV placement and trajectory design for data-gathering in IoT applications. Section III describes the system model and formulates the problem of maximizing the total energy savings of devices. Then, in Sections IV and V, we propose efficient algorithms for solving the device association and UAV placement problems, respectively. In Section VI, the proposed schemes are further modified to enable collision-free scheduling and data-freshness-aware fair association. Section VII presents computer simulations to demonstrate the effectiveness of our proposed scheme. Finally, we conclude the paper in Section VIII.

II. Related Work

The use of UAVs in wireless communications has been examined recently for both cellular and IoT applications. For systems with only a single UAV, the task is often focused on determining the optimal UAV placement or trajectory design to optimize the communication performance (such as throughput or energy efficiency) or to minimize the cost (such as energy consumption or delay). In terms of UAV placement, [21] derived the optimal altitude that yields the maximum coverage radius for a single UAV by taking into consideration the LoS probability at different elevation angles. Similarly, [22] determined the optimal 3D placement of a UAV BS by maximizing the number of ground users that are covered. In terms of trajectory design, [6] studied the throughput maximization problem for a single UAV relay between a fixed source and destination by optimizing the relay trajectory and the source/relay transmit power over a finite horizon. Reference [23] further took into consideration the UAV's propulsion energy consumption and optimized the flight trajectory by maximizing the energy efficiency in bits/Joule. A propulsion energy consumption model for fixed-wing UAVs was derived as a function of the flying velocity and acceleration. A similar energy minimization problem was studied in [24] for a rotary-wing UAV. Moreover, [25] investigated the optimal deployment and movement of a single UAV for supporting downlink wireless communications in the presence of underlaid device-to-device links. The authors provided an analytical framework for the coverage and sum rate using tools from stochastic geometry, and found the minimum number of stop points required to cover a given area. Trajectory design and resource allocation problems can also be studied for downlink data dissemination

Authorized licensed use limited to: National Tsing Hua Univ.. Downloaded on March 09,2022 at 07:46:55 UTC from IEEE Xplore. Restrictions apply.

and energy harvesting applications, as done in [26] and [27], where the UAV was respectively treated as the data source and the dedicated RF energy source.

For data gathering applications in IoT and WSNs (in addition to the works mentioned in the previous section, i.e., [10]–[15]), [28] proposed to minimize the UAV's power consumption by jointly optimizing the sensors' transmission schedule, power allocation, and UAV's flight trajectory while satisfying the sensors' transmission rate requirements. Reference [29] proposed to collect the data from as many sensor nodes as possible in order to minimize the mean squared error of the underlying parameter estimate subject to practical mobility constraints. Moreover, [30] and [17] examined the use of UAV for data-gathering from backscatter sensor devices. The former studied the UAV's trajectory design with the goal of minimizing the mean-squared error of the reconstructed sensor observations, whereas the latter proposed a joint trajectory design, device scheduling, and carrier emitter transmit power control policy by maximizing the energy efficiency of the system. Furthermore, [31] proposed a priority-based frame selection scheme that allows sensors in the rear-side of a forward-moving UAV to transmit with higher priority.

For systems with multiple UAVs, several recent works investigated the joint placement or trajectory design of the UAVs under similar optimizing criteria. Specifically, [16] maximized the minimum throughput of all ground users in the downlink by jointly optimizing the multiuser scheduling, association, and the multiple UAVs' trajectory and power control. In the uplink, [32] jointly optimized the 3D placement of UAVs and user association by maximizing the aggregate throughput of all users under bandwidth limitations and quality-of-service constraints. The problem was broken down into three separate sub-problems to facilitate implementation in a distributed fashion. Reference [33] considered the use of multiple UAVs for the relaying of information from ground users over a non-orthogonal multiple access (NOMA) channel. Both UAV deployment and user pairing schemes were examined for the proposed uplink scenario, as well as a sum power minimization based resource allocation algorithm. Moreover, [34] examined the deployment of multiple rotary-wing UAVs using a quantization theory approach that aims to minimize the average transmission power of ground terminals under both static and dynamic user densities. Reference [35] instead focused on the fast deployment of UAVs to ensure coverage over the region of interest. Two fast deployment algorithms were proposed based on the minimization of the maximum and the total deployment delays, respectively, taking into consideration the UAVs' different flying speeds, operating altitudes, and wireless coverage radius. Reference [36] studied the joint trajectory and power control problem for a downlink multi-UAV interference channel, where the aggregate sum rate of the multiple UAV to ground terminal pairs are maximized. Furthermore, [37] examined the optimal deployment as well as the cyclic recharging and reshuffling of multiple UAVs for providing long-term coverage in cellular networks. The solutions were obtained by maximizing an energy-efficiency-based objective subject to a seamless coverage constraint.

For data gathering applications in WSNs, [38] proposed a joint trajectory design for multiple UAVs by minimizing the maximum mission completion time, as well as the wake-up scheduling and association for sensors, while ensuring that the upload request of all sensors is satisfied with a given energy budget. Reference [39] considered a time-sensitive sensor network where each sensor has its own latency requirement. In this case, a priority-oriented trajectory planning problem was examined and a solution was proposed using a deep Q-learning network. Reference [40] considered the joint trajectory design of multiple UAVs by minimizing the maximum flight time of UAVs such that all sensors' data is collected by the UAVs and transported to the BS. Reference [41] determined the dynamic positioning of multiple UAVs by maximizing the value of the sensor information that is gathered in real-time using particle swarm optimization. The value of the sensor information depends on the sensor type and the elapsed time after the previous sensing time.

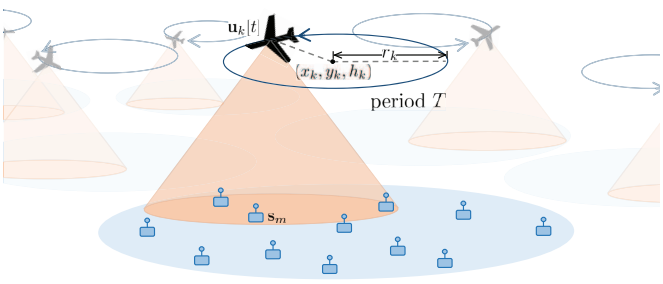

Fig. 1. Illustration of multiple fixed-wing UAVs.

Different from the above works, we focus on the placement of fixed-wing UAVs that follow circular trajectories to gather data from the associated ground devices. The solution must take into account the relative distances between the devices and the UAVs' positions on their circular trajectories. Notice that the simple K-means clustering, which places each UAVs' trajectory center at the centroid position of its associated devices, is not a suitable solution in this case. We argue that the circular trajectory is also more robust compared to most works that adapt their designs to real-time changes in the environment.

III. System Model and Problem Formulation

Let us consider an IoT network with M devices deployed on the ground over a bounded region of interest, and K fixed-wing UAVs circling above their respective coverage regions, as illustrated in Fig. 1. The devices and UAVs are denoted by the sets $\mathcal{M} = \{1, \ldots, M\}$ and $\mathcal{K} = \{1, \ldots, K\}$, respectively. The locations of ground devices are assumed to be fixed whereas those of fixed-wing UAVs vary constantly over time. Therefore, the location of ground device $m \in \mathcal{M}$ is denoted by the 3D coordinates $\mathbf{s}_m = (s_{m,1}, s_{m,2}, s_{m,3})$, and the location of UAV $k \in \mathcal{K}$ at time t is denoted by $\mathbf{u}_k[t] = (u_{k,1}[t], u_{k,2}[t], u_{k,3}[t])$. Here, we assume that the altitudes of the ground devices are 0 (i.e., $s_{m,3} = 0$, $\forall m$), but the work can be easily adapted to cases that take into consideration varying heights of the terrain. Different from rotary-wing UAVs [1], fixed-wing UAVs must be constantly moving in order to stay afloat. In our case, we assume that each UAV follows a circular flight trajectory with period T

Authorized licensed use limited to: National Tsing Hua Univ.. Downloaded on March 09,2022 at 07:46:55 UTC from IEEE Xplore. Restrictions apply.

above their respective coverage region. Hence, the location of UAV k at time t can be expressed as

$$\mathbf{u}_k[t] = (x_k + r_k \cos(2\pi t/T),\ y_k + r_k \sin(2\pi t/T),\ h_k), \tag{1}$$

where (x_k, y_k) represents the two-dimensional center coordinates of the circular trajectory of UAV k on the horizontal plane, h_k is the altitude, and r_k is the radius.

We consider an uplink scenario in which each IoT device is associated with at most one UAV, and the transmissions of IoT devices occur over orthogonal channels. In particular, the IoT devices associated with the same UAV are scheduled to transmit in orthogonal time intervals whereas those associated with different UAVs transmit over different frequency bands. The association between devices and UAVs are described by the binary association variables $a_{m,k}$, for $m = 1, \ldots, M$ and $k = 1, \ldots, K$, where $a_{m,k} = 1$ if device m is associated with UAV k and $a_{m,k} = 0$, otherwise. Moreover, we have $\sum_{k=1}^{K} a_{m,k} \leq 1$, for all m. The traffic demand of device m is given by λ_m in terms of the number of bits per flight cycle T, and the maximum number of bits that UAV k can receive over time T (i.e., the capacity limit of UAV k) is given by μ_k. In this case, device m must occupy λ_m/μ_k fraction of the time available for transmission to UAV k in each flight cycle (i.e., $\frac{\lambda_m}{\mu_k} T$). Moreover, we say that the transmission from device m to UAV k at time t is successful if the receive SNR at this time exceeds the threshold γ_k.

A. Ground-to-Air Path Loss Model

Let $P_m[t] \in [0, P_{\max}]$ be the transmission power of device m at time t, where $P_{\max}$ is the maximum transmission power of each device. Then, the signal-to-noise ratio (SNR) between device m and UAV k at time t can be written as

$$\mathrm{SNR}_m(\mathbf{u}_k[t]) \triangleq \frac{P_m[t]}{\overline{\mathrm{PL}}_m(\mathbf{u}_k[t])\sigma_k^2}, \tag{2}$$

where $\overline{\mathrm{PL}}_m(\mathbf{u}_k[t])$ is the path loss between device m and UAV k, and σ_k^2 is the noise variance at UAV k. Following the ground-to-air path loss model in [21], which takes into consideration the probability of line-of-sight (LoS) between the ground device and the UAV based on their relative locations, the path loss can be expressed (in dB) as

$$\begin{aligned}\left(\overline{\mathrm{PL}}_m(\mathbf{u}_k[t])\right)_{\mathrm{dB}} &= 10\log_{10}\left(\frac{4\pi f_c}{c}\right)^2 \\ &\quad + 10\log_{10}\|\mathbf{s}_m - \mathbf{u}_k[t]\|^{\alpha} \\ &\quad + \eta_{\mathrm{LoS}}\,\rho_{m,\mathrm{LoS}}(\mathbf{u}_k[t]) \\ &\quad + \eta_{\mathrm{NLoS}}\left[1 - \rho_{m,\mathrm{LoS}}(\mathbf{u}_k[t])\right]\end{aligned} \tag{3}$$

where f_c is the carrier frequency, c is the speed of light, α is the path loss coefficient, η_{LoS} and η_{NLoS} are the excessive path loss coefficients corresponding to LoS and NLoS links, respectively, and $\rho_{m,\mathrm{LoS}}(\mathbf{u}_k[t])$ is the probability of LoS between device m and UAV k at time t. The LoS probability can be approximated as [21]

$$\rho_{m,\mathrm{LoS}}(\mathbf{u}_k[t]) = \frac{1}{1 + \psi \exp\{-\beta[\theta_m(\mathbf{u}_k[t]) - \psi]\}}, \tag{4}$$

where ψ and β are parameters depending on the environment (e.g., rural or urban) and $\theta_m(\mathbf{u}_k[t]) = \frac{180}{\pi}\sin^{-1}(h_k/\|\mathbf{s}_m - \mathbf{u}_k[t]\|)$ is the elevation angle between device m and UAV k at time t. Notice from (4) that, by increasing the flight altitude of UAV k (i.e., h_k), the elevation angle between device m and UAV k increases (which increases the LoS probability), but the transmission distance also increases (which makes the signal decay more severe). Hence, the flight altitudes of the UAVs must be carefully chosen in order to best exploit the trade-off between the LoS probability and the signal decay over distance.

B. Problem Formulation

The main objective of this work is to determine the UAVs' locations (including their 2D center coordinates (x_k, y_k), height h_k, and radius r_k, for all k), and the device association $\{a_{m,k}, \forall m, k\}$ to maximize the energy savings (and, thus, reduce the energy consumption) of the ground IoT devices. To focus on the above issue, we first consider an ideal scheduling scenario where each IoT device is assumed to be able to complete its transmission instantaneously when its associated UAV arrives at its closest point in the flight trajectory. In this case, the distance between device m and UAV k at the closest point is given by

$$\begin{aligned}&\min_{t\in[0,T]} \|\mathbf{s}_m - \mathbf{u}_k[t]\| \\ &\quad = \sqrt{\left\|\left(s_{m,1} - x_k, s_{m,2} - y_k\right)\right\| - r_k)^2 + h_k^2}\end{aligned}$$

and, thus, the path loss between device m and UAV k can be approximated as

$$\begin{aligned}&\left(\overline{\mathrm{PL}}_m(\mathbf{u}_k[t])\right)_{\mathrm{dB}} \\ &\quad \approx \left(\overline{\mathrm{PL}}_m(x_k, y_k, h_k, r_k)\right)_{\mathrm{dB}} \qquad (5) \\ &\quad \triangleq 10\log_{10}\frac{4\pi f_c}{c} \\ &\quad + 10\log_{10}\left[\left(\left\|\left(s_{m,1} - x_k, s_{m,2} - y_k\right)\right\| - r_k\right)^2 + h_k^2\right]^{\frac{\alpha}{2}} \\ &\quad + \eta_{\mathrm{NLoS}} + \frac{\eta_{\mathrm{LoS}} - \eta_{\mathrm{NLoS}}}{1 + \psi\exp\{-\beta[\theta_m(x_k, y_k, h_k, r_k) - \psi]\}} \qquad (6)\end{aligned}$$

where

$$\begin{aligned}&\theta_m(x_k, y_k, h_k, r_k) \\ &\quad \triangleq \frac{180}{\pi}\sin^{-1}\frac{h_k}{\sqrt{\left(\left\|\left(s_{m,1} - x_k, s_{m,2} - y_k\right)\right\| - r_k\right)^2 + h_k^2}}\end{aligned} \tag{7}$$

is the elevation angle at the closest point. Notice that, under the ideal scheduling assumption, the transmission time of each device is predetermined and, thus, the path loss will only depend on the associated UAV's trajectory center and radius (see (5)). The design of practical scheduling policies that can take into consideration the devices' non-negligible transmission intervals and are able to ensure collision-free transmission while minimizing the deviation from the ideal transmission times will be discussed in Section VI.

The proposed UAV deployment and device association problem can thus be formulated as

$$\max_{\substack{x_k, y_k, h_k, r_k,\\ a_{m,k}, P_m, \forall m,k}} \sum_{k=1}^{K}\sum_{m=1}^{M} a_{m,k}\frac{\lambda_m}{\mu_k} T(P_{\max} - P_m), \tag{8a}$$

Authorized licensed use limited to: National Tsing Hua Univ.. Downloaded on March 09,2022 at 07:46:55 UTC from IEEE Xplore. Restrictions apply.

$$\text{subject to} \quad \sum_{k=1}^{K} a_{m,k} \leq 1, \ a_{m,k} \in \{0,1\}, \tag{8b}$$

$$\sum_{m=1}^{M} \lambda_m a_{m,k} \leq \mu_k, \tag{8c}$$

$$\frac{P_m}{\overline{\mathrm{PL}}_m(x_k, y_k, h_k, r_k)\sigma_k^2} \geq a_{m,k}\gamma_k, \tag{8d}$$

$$h_{\min} \leq h_k \leq h_{\max}, \ r_{\min} \leq r_k \leq r_{\max} \tag{8e}$$

$$0 < P_m \leq P_{\max}, \ \forall m, k, \tag{8f}$$

where $\lambda_m T/\mu_k$ represents the time duration required for the transmission between device *m* and UAV *k*, and $P_{\max} - P_m$ is the difference between the maximum and the actual transmission powers of device *m*. Hence, the objective yields the total energy savings that can be experienced by the IoT devices compared to transmitting at maximum power. The constraint in (8b) ensures that each device is associated with at most one UAV, (8c) ensures that the scheduled transmissions are within the capacity limit of each UAV, and (8d) ensures that the transmissions of associated devices are successful in the sense that the target SNR thresholds (i.e., γ_k, for all *k*) are satisfied. The remaining constraints in (8e) and (8f) provide upper and lower bounds to the flight altitude, radius, and transmission power. Note that, different from the conventional total power minimization problem, the maximization of the total energy savings improves both the energy and the association efficiency since only the energy savings of associated devices are accounted for in the objective. The total power minimization problem will instead result in a trivial solution where no devices are associated with any UAV in our case. We assume that the UAV deployment and device association are computed at a central station that has knowledge of the locations and demands of all IoT devices. The solutions are obtained offline before the UAVs are dispatched to perform data-gathering from the devices.

More specifically, in (8), the UAVs' trajectory centers and radii as well as the devices' association decisions and transmission powers are unknowns that are to be solved by maximizing the total energy savings of ground devices. The total energy savings depend on the transmission powers and association decisions of the devices, which can be maximized by associating each device to the UAV that can be reached by the least transmission power. However, from (8d), we can see that the device's minimum transmission power required to reach each UAV is determined by the UAV's trajectory center and radius. Moreover, the association decisions of the devices must also satisfy the capacity constraint in (8f), which causes competition among the devices. This results in a mixed integer nonlinear programming problem with variables that are strongly coupled through the capacity and SNR constraints, which is particularly challenging to solve.

In this work, we propose to solve the device association and the UAV deployment problems in an alternating fashion, where one problem is solved while the solution of the other is fixed. In particular, given the UAVs' trajectory centers and radii, the device association problem is first modeled as a 0-1 multiple knapsack problem with assignment restrictions (MKPAR) [19] and an approximate algorithm is proposed to solve the problem. Then, given the device association, the UAVs' locations are then determined using a weighted averaging of the associated devices' locations. The above two subproblems are solved iteratively until convergence. Notice that, since the total energy savings is increased in each step, the proposed algorithm converges. The solutions proposed for the two subproblems are described separately in the following sections.

IV. Device Association as a 0-1 Multiple Knapsack Problem With Assignment Restrictions

In this section, we examine the device association problem (i.e., the optimization over the binary association variables $\{a_{k,m}, \forall k, m\}$) for fixed UAVs' trajectory centers and radii (i.e., $\{x_k, y_k, h_k, r_k, \forall k\}$). We show that the problem can be modeled as a 0-1 MKPAR problem [19], [20] and propose an approximate algorithm to solve it. The proposed algorithm aims to maximize the IoT devices' energy savings and, thus, is referred to as the maximum energy-saving (MES) device association algorithm.

Specifically, given the trajectory centers and radii (i.e., $\{x_k, y_k, h_k, r_k, \forall k\}$), the problem in (8) reduces to

$$\max_{a_{m,k}, P_m, \forall m,k} \ \sum_{k=1}^{K} \sum_{m=1}^{M} a_{m,k} \frac{\lambda_m}{\mu_k} T(P_{\max} - P_m), \tag{9a}$$

$$\text{subject to} \quad \sum_{k=1}^{K} a_{m,k} \leq 1, \ a_{m,k} \in \{0,1\}, \tag{9b}$$

$$\sum_{m=1}^{M} \lambda_m a_{m,k} \leq \mu_k, \tag{9c}$$

$$a_{m,k}\tilde{\gamma}_{m,k} \leq P_m \leq P_{\max}, \tag{9d}$$

where $\tilde{\gamma}_{m,k} \triangleq \gamma_k \sigma_k^2 \overline{\mathrm{PL}}_m(x_k, y_k, h_k, r_k)$ is the minimum required transmission power of device *m* when it is associated with UAV *k*. This problem can be viewed as a 0-1 MKPAR problem where each UAV, say UAV *k*, is a knapsack with capacity μ_k, and each device, say device *m*, is an item with weight λ_m. The capacity of a knapsack represents the maximum total weight of items that it can accommodate. Here, the assignment of item *m* to knapsack *k* is said to yield profit $\frac{\lambda_m}{\mu_k} T(P_{\max} - \tilde{\gamma}_{m,k})$, which represents the energy savings of device *m* per flight cycle. However, to satisfy the constraint in (9d), the assignment to UAV *k* in this case must be restricted to the set $\mathcal{M}_k \triangleq \{m \in \mathcal{M} : \tilde{\gamma}_{m,k} < P_{\max}\}$, which consists of devices within the communication range of UAV *k* and, thus, can potentially be associated with the UAV. Consequently, the device association problem in (9) becomes equivalent to the profit-maximization problem in MKPAR.

To solve the MKPAR problem, we propose an approximate algorithm that involves solving the basic 0-1 single knapsack problem [20] in parallel for all UAVs followed by a profit-based reassignment policy to resolve conflict among UAVs. The algorithm can be summarized into two stages.

Stage 1 (0-1 Single Knapsack Problem): In Stage 1, each UAV aims to solve the basic 0-1 single knapsack problem individually without consideration of other UAVs. In particular, each UAV, say UAV *k*, seeks to find the set of devices that it hopes to be associated with, i.e., the set

$$\mathcal{A}_k^* = \underset{\mathcal{A}_k \subset \mathcal{M}_k : \sum_{m \in \mathcal{A}_k} \lambda_m \leq \mu_k}{\arg\max} \ \sum_{m \in \mathcal{A}_k} \frac{\lambda_m}{\mu_k} T\big(P_{\max} - \tilde{\gamma}_{m,k}\big). \tag{10}$$

Authorized licensed use limited to: National Tsing Hua Univ.. Downloaded on March 09,2022 at 07:46:55 UTC from IEEE Xplore. Restrictions apply.

Algorithm 1 MES Device Association Algorithm

Initialize: $a_{m,k}=0$, for all m and k, and $\mathcal{M}_k=\{m\in\mathcal{M}:\tilde{\gamma}_{m,k}<P_{\max}\}$.
while $\mu_k\geq\min_{m\in\mathcal{M}_k}\lambda_m$, for some k **do**
  for $k=1$ to K **do**
    Find $\mathcal{A}_k^*$ by (10) using dynamic programming.
  end for
  for $k=1$ to K **do**
    Update $a_{m,k}$ according to (26), for all $m\in\mathcal{M}_k$.
  end for
  Update $\mu_k\leftarrow\mu_k-\sum_{m\in\mathcal{M}_k}\lambda_m a_{m,k}$ and $\mathcal{M}_k\leftarrow\mathcal{M}_k\setminus\left\{m\in\mathcal{M}_k:\sum_{k'=1}^{K}a_{m,k'}=1\right\}$, for all k.
end while
return $\{a_{m,k},\forall m,k\}$

This problem can be solved by dynamic programming [42], which yields computational complexity given by $O(M\mu_k)$ [42] for UAV k. By considering the complexity of all K UAVs, the worst-case complexity of Stage 1 is given by $O(MK\mu_{\max})$, where $\mu_{\max}=\max_{k\in\mathcal{K}}\mu_k$. However, at the end of this stage, the subsets $\{\mathcal{A}_k^*\}_{k=1}^K$ may overlap with each other and, thus, must be resolved in order to satisfy the association constraint in (9b).

Stage 2 (Maximum Profit Assignment): In Stage 2, the devices that are simultaneously chosen by more than one UAV are resolved by associating each device to the UAV that yields the maximum profit. That is, we set

$$a_{m,k}=\begin{cases}1, & \text{for } k=\underset{k':\,m\in\mathcal{A}_{k'}^*}{\arg\max}\ \frac{\lambda_m}{\mu_k}T\big(P_{\max}-\tilde{\gamma}_{m,k'}\big),\\ 0, & \text{otherwise,}\end{cases}\tag{11}$$

for all $m\in\mathcal{M}_k$ and for all k. This requires each device to scan over the profits (i.e., the energy-savings) associated with each of the K UAVs. Therefore, the aggregate complexity over all devices is given by $O(KM)$.

Notice that, after Stage 2, UAVs that fail to associate with some of their originally chosen devices may have remaining capacity to serve other devices that have not yet been chosen by any of the UAVs. Hence, to fully utilize the remaining capacity of the UAVs, we repeat the two stages again with the updated UAV capacities and sets of connectable devices given by

$$\mu_k\leftarrow\mu_k-\sum_{m\in\mathcal{M}_k}\lambda_m a_{m,k},\tag{12}$$

and

$$\mathcal{M}_k\leftarrow\mathcal{M}_k\setminus\left\{m\in\mathcal{M}_k:\ \sum_{k'=1}^{K}a_{m,k'}=1\right\},\tag{13}$$

respectively, for all k. In particular, (12) updates the remaining capacity of UAV k by subtracting the capacity μ_k by the demand of devices that have been successfully associated with UAV k in the current iteration, i.e., $\sum_{m\in\mathcal{M}_k}\lambda_m a_{m,k}$. Then, (13) updates the remaining set of devices in the range of UAV k that have not yet been associated with any of the UAVs. This is done by subtracting $\mathcal{M}_k$ by the set of devices that have been associated with one of the UAVs in the current iteration, i.e., $\{m\in\mathcal{M}_k:\ \sum_{k'=1}^{K}a_{m,k'}=1\}$. The process is repeated until no further assignment is possible. The algorithm is summarized in Algorithm 1.

V. Load-Balancing UAV Deployment and Flight Radius Adjustment

In this section, we examine the optimal trajectory centers and radii of the UAVs (i.e., x_k, y_k, h_k, and r_k, for all k) for given device association decisions and the respective transmission powers of the devices (i.e., $a_{m,k}$ and P_m, for all m and k). In this case, the constraints in (8b), (8c), (8d), and (8f) become irrelevant to the optimization and can be removed. The variable P_m can also be replaced with the minimum required transmission power $\tilde{\gamma}_{m,k}$, for each k. Therefore, given the device association policy, the optimization problem in (8) can be reduced to the following

$$\max_{x_k,y_k,h_k,r_k\forall k}\ \sum_{k=1}^{K}\sum_{m=1}^{M}a_{m,k}\frac{\lambda_m}{\mu_k}T\big(P_{\max}-\tilde{\gamma}_{m,k}\big),\tag{14a}$$

$$\text{subject to}\ \ h_{\min}\leq h_k\leq h_{\max},\tag{14b}$$

$$r_{\min}\leq r_k\leq r_{\max},\ \forall k.\tag{14c}$$

Since the objective is additive and the constraints for different UAVs are separate, the problem can be decoupled into K parallel weighted sum power minimization subproblems, one for each UAV. The weighted sum power minimization subproblem of UAV k can be written as

$$\min_{x_k,y_k,h_k,r_k}\ \sum_{m=1}^{M}a_{m,k}\lambda_m\tilde{\gamma}_{m,k}(x_k,y_k,h_k,r_k),\tag{15a}$$

$$\text{subject to}\ \ h_{\min}\leq h_k\leq h_{\max},\tag{15b}$$

$$r_{\min}\leq r_k\leq r_{\max},\tag{15c}$$

where $\tilde{\gamma}_{m,k}(x_k,y_k,h_k,r_k)$ is expressed as a function of (x_k,y_k,h_k,r_k) to emphasize its dependence on these variables. Here, we propose to solve this problem by an approximate coordinate descent algorithm which leads to an insightful iterative load-balancing (ILB) procedure.

For notational simplicity, we express the vector of optimizing parameters as $\boldsymbol{\phi}_k\triangleq(x_k,y_k,h_k,r_k)$. Then, by (6) and by removing the terms not relevant to m or $\boldsymbol{\phi}_k$, the objective function in (15) can be simplified as

$$J\ (\boldsymbol{\phi}_k)\triangleq\sum_{m=1}^{M}a_{m,k}\Psi_m(\boldsymbol{\phi}_k)\times\left[\left(\sqrt{(s_{m,1}-x_k)^2+(s_{m,2}-y_k)^2}-r_k\right)^2+h_k^2\right]\tag{16}$$

where $\Psi_m(\boldsymbol{\phi}_k)\triangleq\lambda_m 10^{\frac{(\eta_{\text{LoS}}-\eta_{\text{NLoS}})/10}{1+\psi\exp\{-\beta[\theta_m(x_k,y_k,h_k,r_k)-\psi]\}}}$ is determined by the LoS probability model in (4) (i.e., [21]) and depends on the load demand λ_m. Notice that, the larger is the elevation angle (i.e., the closer is the device to the closest trajectory point), the smaller the value of $\Psi_m(\boldsymbol{\phi}_k)$ since $\eta_{\text{LoS}}<\eta_{\text{NLoS}}$. Suppose that $\boldsymbol{\phi}^{(\ell)}\triangleq(x_k^{(\ell)},y_k^{(\ell)},h_k^{(\ell)},r_k^{(\ell)})$ is the solution obtained in the ℓ-th iteration of the proposed iterative algorithm. Then, in iteration $\ell+1$, the variables x_k and y_k can be updated as

$$x_k^{(\ell+1)}=x_k^{(\ell)}-\eta\frac{\partial J\left(\boldsymbol{\phi}_k^{(\ell)}\right)}{\partial x_k^{(\ell)}}\tag{17}$$

Authorized licensed use limited to: National Tsing Hua Univ.. Downloaded on March 09,2022 at 07:46:55 UTC from IEEE Xplore. Restrictions apply.

Algorithm 2 ILB UAV Deployment and Radius Adjustment Algorithm (for UAV k)

1: **Initialize:** Set $\ell = 0$ and the initial values of
2: **while** $\|\boldsymbol{\phi}_k^{(\ell+1)} - \boldsymbol{\phi}_k^{(\ell)}\| / \|\boldsymbol{\phi}_k^{(\ell)}\| > \epsilon$ **do**
3: Update the center coordinates as

$$x_k^{(\ell+1)} \approx (1-\alpha) x_k^{(\ell)} + \alpha \tilde{x}_k^{(\ell+1)},$$
$$y_k^{(\ell+1)} \approx (1-\alpha) y_k^{(\ell)} + \alpha \tilde{y}_k^{(\ell+1)},$$

where $\tilde{x}_k^{(\ell+1)}$ and $\tilde{y}_k^{(\ell+1)}$ are the load-balancing coordinates defined in (23) and (25), respectively.
4: Update $h_k^{(\ell+1)}$ and $r_k^{(\ell+1)}$, as in (26), by a two-dimensional line search.
5: **end while**

and

$$y_k^{(\ell+1)} = y_k^{(\ell)} - \eta \frac{\partial J\left(\boldsymbol{\phi}_k^{(\ell)}\right)}{\partial y_k^{(\ell)}}. \tag{18}$$

In particular, the partial derivative with respect to x_k at point $x_k^{(\ell)}$ can be written as

$$\frac{\partial J\left(\boldsymbol{\phi}_k^{(\ell)}\right)}{\partial x_k^{(\ell)}} = \sum_{m=1}^{M} a_{m,k} \Bigg\{ -2\Psi_m\left(\boldsymbol{\phi}_k^{(\ell)}\right)\left(s_{m,1} - x_k^{(\ell)}\right) \cdot \left(1 - \frac{r_k^{(\ell)}}{\sqrt{(s_{m,1} - x_k^{(\ell)})^2 + \left(s_{m,2} - y_k^{(\ell)}\right)^2}}\right) + \frac{\partial \Psi_m\left(\boldsymbol{\phi}_k^{(\ell)}\right)}{\partial x_k^{(\ell)}} \cdot \left[\left(\sqrt{\left(s_{m,1} - x_k^{(\ell)}\right)^2 + \left(s_{m,2} - y_k^{(\ell)}\right)^2} - r_k^{(\ell)}\right)^2 + \left(h_k^{(\ell)}\right)^2\right]\Bigg\} \tag{19}$$

Notice that, for h_k sufficiently large, small changes in the UAV's horizontal position would not have a significant impact on the elevation angle and, thus, we can assume that $\frac{\partial \Psi_m(\boldsymbol{\phi}_k)}{\partial x_k}$ is small and that the second term is negligible. In this case, the derivative can be approximated as

$$\frac{\partial J\left(\boldsymbol{\phi}_k^{(\ell)}\right)}{\partial x_k^{(\ell)}} \approx -2 \sum_{m=1}^{M} a_{m,k} \tilde{\Psi}_m\left(\boldsymbol{\phi}_k^{(\ell)}\right)\left(s_{m,1} - x_k^{(\ell)}\right) \tag{20}$$

where $\tilde{\Psi}_m(\boldsymbol{\phi}_k) \triangleq \Psi_m(\boldsymbol{\phi}_k)\left(1 - \frac{r_k}{\sqrt{(s_{m,1}-x_k)^2 + (s_{m,2}-y_k)^2}}\right)$. Then, the coordinate descent update of x_k in iteration $\ell + 1$ can be approximated as

$$x_k^{(\ell+1)} \approx x_k^{(\ell)} + 2\eta \sum_{m=1}^{M} a_{m,k} \tilde{\Psi}_m\left(\boldsymbol{\phi}_k^{(\ell)}\right)\left(s_{m,1} - x_k^{(\ell)}\right). \tag{21}$$

Moreover, by choosing $\eta = \frac{\alpha}{2\sum_{m'=1}^{M} a_{m',k} \tilde{\Psi}_{m'}(\boldsymbol{\phi}_k^{(\ell)})}$, we have

$$x_k^{(\ell+1)} \approx (1-\alpha) x_k^{(\ell)} + \alpha \tilde{x}_k^{(\ell+1)}, \tag{22}$$

where

$$\tilde{x}_k^{(\ell+1)} \triangleq \sum_{m=1}^{M} \frac{a_{m,k} \tilde{\Psi}_m\left(\boldsymbol{\phi}_k^{(\ell)}\right)}{\sum_{m'=1}^{M} a_{m',k} \tilde{\Psi}_{m'}\left(\boldsymbol{\phi}_k^{(\ell)}\right)} s_{m,1} \tag{23}$$

is a weighted sum of the x-coordinates of devices associated with UAV k. Similarly, the update of y_k in iteration $\ell + 1$ can be approximated as

$$y_k^{(\ell+1)} \approx (1-\alpha) y_k^{(\ell)} + \alpha \tilde{y}_k^{(\ell+1)}, \tag{24}$$

where

$$\tilde{y}_k^{(\ell+1)} \triangleq \sum_{m=1}^{M} \frac{a_{m,k} \tilde{\Psi}_m\left(\boldsymbol{\phi}_k^{(\ell)}\right)}{\sum_{m'=1}^{M} a_{m',k} \tilde{\Psi}_{m'}\left(\boldsymbol{\phi}_k^{(\ell)}\right)} s_{m,2}. \tag{25}$$

It is interesting to observe that, in iteration $\ell + 1$, UAV k is moved horizontally towards the position $(\tilde{x}_k^{(\ell+1)}, \tilde{y}_k^{(\ell+1)})$, which is a weighted sum of the 2D coordinates of the associated devices. In fact, since the weights, i.e., $\{\tilde{\Psi}_m(\boldsymbol{\phi}_k^{(\ell)})\}_{m=1}^{M}$, are proportional to the load demands of the corresponding devices (i.e., $\{\lambda_m\}_{m=1}^{M}$), the proposed UAV deployment policy places more emphasis on devices with higher load demands. Hence, we refer to this algorithm as the iterative load-balancing (ILB) algorithm. Moreover, we can see that $\tilde{\Psi}_m(\boldsymbol{\phi}_k^{(\ell)})$ is positive if $\sqrt{(s_{m,1} - x_k)^2 + (s_{m,2} - y_k)^2} > r_k$ (i.e., if device m is outside the UAV's circular flight trajectory), and is negative, otherwise (i.e., if device m is inside the circular trajectory). In the former case, moving the trajectory center closer to device m reduces the transmission distance between device m and the closest point on the UAV's trajectory, and vice versa in the latter case. This effect is unique to circling fixed-wing UAVs and is not captured by the simple K-means deployment often adopted in the literature for rotary-wing UAVs.

Following similar arguments, we can also obtain gradient updates for the altitude and radius of each UAV. However, since both the altitude and the radius are confined within finite intervals, namely, $[h_{\min}, h_{\max}]$ and $[r_{\min}, r_{\max}]$, respectively, we instead replace the gradient updates of these parameters with a simple two-dimensional line search. That is, in iteration $\ell+1$, the altitude and radius of UAV k can also be updated by solving the optimization problem in (15) for fixed $(x_k, y_k) = (x_k^{(\ell+1)}, y_k^{(\ell+1)})$. In this case, we have

$$\left(h_k^{(\ell+1)}, r_k^{(\ell+1)}\right) = \underset{\substack{h_k \in [h_{\min}, h_{\max}] \\ r_k \in [r_{\min}, r_{\max}]}}{\arg\min} \sum_{m=1}^{M} a_{m,k} \lambda_{m,k} \tilde{\gamma}_{m,k} \times \left(x_k^{(\ell+1)}, y_k^{(\ell+1)}, h_k, r_k\right), \tag{26}$$

where the solution is obtained by line search. The complexity of the 2D line search for each UAV is $O(1/\varepsilon^2)$, where ε is the resolution of the line search on each dimension. The above procedures are repeated until no further improvement can be observed in terms of the weighted sum transmit power, as described in (15a). The computational complexity at each UAV is dominated by the line search and, thus, is given by $O(N_{\text{iter}}/\varepsilon^2)$, where N_{iter} is the number of iterations required until convergence. Note that, by setting the convergence criterion as $\|\boldsymbol{\phi}_k^{(\ell+1)} - \boldsymbol{\phi}_k^{(\ell)}\| / \|\boldsymbol{\phi}_k^{(\ell)}\| > \epsilon$ with $\epsilon = 0.001$ in our experiments (see Section VII), the algorithm typically converges within 11 iterations. The algorithm is summarized in Algorithm 2. It is worthwhile to note that, while it may be possible to alternate between Algorithms 1 and 2

Authorized licensed use limited to: National Tsing Hua Univ.. Downloaded on March 09,2022 at 07:46:55 UTC from IEEE Xplore. Restrictions apply.

until convergence, our experiments show that little advantage can be gained by doing so. Hence, we propose to perform Algorithms 1 and 2 only once in order to reduce the system complexity.

Here, we assume that the above solutions are computed offline with central knowledge of the locations and demands of all IoT devices that remain static over time. However, we argue that it is also possible to implement the algorithms in a distributed fashion by the UAVs. In particular, in the MES device association algorithm, each UAV first solves a separate 0-1 knapsack problem with knowledge of the demands of devices within its vicinity in Stage 1. The distributed association decisions can then be broadcast to the devices where conflict is resolved by selecting the maximum profit UAV. In the ILB UAV deployment and radius adjustment algorithm, the UAVs' trajectory centers and radii are updated independently at the respective UAVs given the current association decisions. The above procedures are suitable for IoT or sensor network applications where the sensor devices feedback their observations periodically over time at fixed transmission rates and locations. Even though the proposed algorithms may be performed in a distributed fashion, they may not be applicable to a mobile environment where the devices' locations and demands may vary rapidly over time.

VI. Collision-Free Scheduling and Data Freshness Aware Association

In the previous sections, the MES and ILB algorithms were proposed for device association and UAV deployment, respectively, based on the optimization problem in (8). However, to simplify the design, we considered an ideal schedule, where the devices were assumed to transmit instantaneously whenever their associated UAVs arrive at the closest points to these devices (see Section III-B). In practice, the devices' transmission durations are non-negligible, and thus the transmissions from close-by devices may collide under ideal scheduling. Moreover, the MES device association algorithm is concerned with only the total energy savings, but does not consider the fairness of devices, especially when the network is overloaded. In this section, we propose effective approaches to achieve collision-free scheduling and enable fair device association through the consideration of data freshness at the UAVs.

A. MES Device Association With Collision-Free Scheduling

Recall that, under the ideal scheduling described in Section III-B, a device, say device m, that is associated with UAV k will be scheduled to transmit at time $t_m^* \triangleq \arg\min_{t\in[0,T]} \|\mathbf{s}_m - \mathbf{u}_k[t]\|$ within each period. The position of UAV k at this time can be written as

$$\mathbf{u}_k[t_m^*] = (x_k + r_k \cos\theta_m^*,\ y_k + r_k \sin\theta_m^*,\ h_k) \quad (27)$$

where $\theta_m^* \triangleq 2\pi t_m^*/T \mod 2\pi$ is the trajectory phase associated with the ideal transmission time instant of device m. We shall refer to θ_m^* as the ideal transmission phase of device m, which is also the phase of the vector from the UAV's trajectory center to device m's location, as illustrated in Fig. 2(a). Moreover, with demand λ_m, device m must occupy λ_m/μ_k fraction of the time available for transmission to UAV k in each flight cycle (i.e., $\frac{\lambda_m}{\mu_k} T$). By taking the non-negligible transmission time into consideration, the transmission of device m should ideally occur over the duration $[t_m^* - \frac{\lambda_m}{\mu_k}\frac{T}{2}, t_m^* + \frac{\lambda_m}{\mu_k}\frac{T}{2}]$ in order to minimize its transmission power. The corresponding trajectory phase interval is then given by $[\theta_m^* - \frac{\lambda_m}{\mu_k}\pi, \theta_m^* + \frac{\lambda_m}{\mu_k}\pi]$. However, for devices with similar ideal transmission phases, their transmission durations are likely to overlap, resulting in collision among devices, as illustrated in Fig. 2(a). Therefore, in practice, it is necessary to adjust the transmission phases of the associated devices (i.e., their actual transmission times within each flight cycle) to avoid collision, albeit at the cost of increased transmission power, as illustrated in Fig. 2(b). Instead of choosing the transmission time to directly maximize the energy savings as in (8), which is difficult to solve in general, we propose a low-complexity solution that aims to minimize the devices' total offset between their ideal and actual transmission phases. The optimization can be done separately for each UAV.

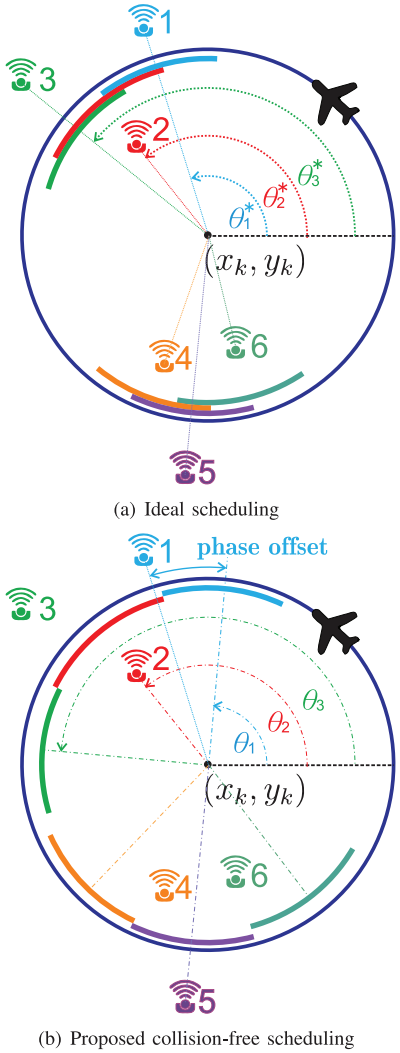

(a) Ideal scheduling

(b) Proposed collision-free scheduling

Fig. 2. Example of the ideal and the proposed collision-free scheduling.

In particular, let us consider the scheduling of devices associated with UAV k. For ease of exposition, we relabel the devices associated with UAV k as devices $1, 2, \ldots, M_k$ in the increasing order of their ideal transmission phases such that $\theta_1^* \le \theta_2^* \le \cdots \le \theta_{M_k}^*$. Then, given the device association $a_{m,k}$, for all m, we formulate the collision-free scheduling problem of UAV k as the following minimum transmission

Authorized licensed use limited to: National Tsing Hua Univ.. Downloaded on March 09,2022 at 07:46:55 UTC from IEEE Xplore. Restrictions apply.

phase offset problem

$$\min_{\theta_m, \forall m} \sum_{m=1}^{M_k} |\theta_m - \theta_m^*| \tag{28a}$$

$$\text{subject to } \theta_{m+1} - \theta_m \geq \frac{\pi}{\mu_k}(\lambda_m + \lambda_{m+1}),$$

$$\text{for } m = 1, \ldots, M_k - 1 \tag{28b}$$

$$\theta_1 + 2\pi - \theta_{M_k} \geq \frac{\pi}{\mu_k}\left(\lambda_1 + \lambda_{M_k}\right). \tag{28c}$$

Notice that, $|\theta_m - \theta_m^*|$ is the absolute difference between the actual and ideal transmission phases of device *m*. Moreover, the constraints ensure that the spacing between the transmission phases are sufficient to accommodate the transmission durations of consecutively scheduled devices. The optimization problem in (28) is convex and, thus, can be solved by a variety of methods [43], including interior point or constrained subgradient algorithms. For example, by adopting the barrier method for the interior point algorithm, the complexity scales as $O(\sqrt{M})$ [43], where *M* is the number of devices (and, thus, the number of constraints).

B. Fair Device Association via Data Freshness Weighting

In addition to the collision-free scheduling, we further consider the fairness of the proposed MES device association algorithm by taking into account the freshness of the data gathered by the UAV. Recall that, in the original MES device association policy, only devices that contribute more to the total energy savings are allowed to associate with the UAVs. Devices that are located far away from the UAVs' flight trajectories or have low demand are less likely to be chosen. As long as the devices' locations do not change, these devices will never be given the opportunity to transmit. To alleviate this problem, we propose a fair alternative of the MES algorithm based on the freshness of the data gathered by the UAVs [44].

Notice that, in IoT applications, devices are often tasked to observe and feedback information (e.g., temperature) about their local environment in a periodic manner. If the information observed in the current period (with duration *T*) is not successfully fed back to the UAV, the data available at the UAV (or the remote data-gathering node) will become additionally outdated by time *T*. To take the data freshness into consideration, we propose to record the outdatedness of device *m*'s observation at the UAV by time T_m. Then, the device association can be dynamically adjusted in each period by solving again the optimization in (9) with a modified objective given by

$$\sum_{k=1}^{K}\sum_{m=1}^{M} a_{m,k}\frac{\lambda_m}{\mu_k} T(P_{\max} - P_m) e^{\varphi_m T_m}, \tag{29}$$

where $\varphi_m > 0$ is the freshness parameter associated with device *m*. Notice that, φ_m determines the importance of device *m*'s data freshness. The data freshness weighting $e^{\varphi_m T_m}$, for all *m*, allows devices to transmit with higher priority if they have not transmitted for a longer time compared to other devices. The outdatedness T_m is increased by one if each device *m* is not successfully associated with a UAV in the current transmission period *T*. The problem can be solved following the procedures in Sections IV and V.

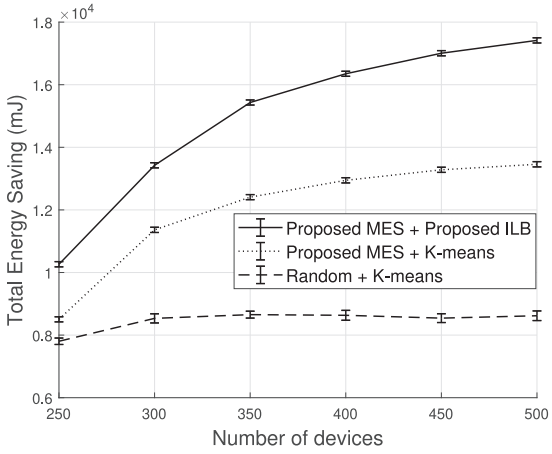

Fig. 3. Total energy savings versus number of devices.

VII. Simulation Results

In this section, we demonstrate the effectiveness of the proposed MES device association and the ILB UAV deployment and radius adjustment algorithms. In the experiments, IoT devices are deployed randomly according to a uniform distribution within a 600 × 600 m^2 area. For the LoS probability in (4), we consider an urban environment with $\psi = 11.95$ and $\beta = 0.14$ at 2 GHz carrier frequency. The period of the flight cycle is set as $T = 34$ seconds, and the minimum and maximum altitude of UAVs are $h_{\min} = 100$ and $h_{\max} = 300$ meters, respectively. The excessive path loss for LoS and NLoS are chosen as $\eta_{\text{LoS}} = 3$ dB and $\eta_{\text{NLoS}} = 23$ dB. The noise power is -82dBm, the SNR threshold is $\gamma_k = 10$ dB, for all *k*, and $P_{\max} = 50$ mW. The altitudes of all UAVs are initialized as $h_{\max}$ to ensure high coverage of ground devices. The load demand of devices (i.e., $\{\lambda_m\}_{m=1}^{M}$) are chosen randomly according to a uniform distribution between [1, 10] units, and the capacity limits of the UAVs are set as $\mu_k = 500$ units, $\forall k$. The following results are averaged over 100 different network realizations.

In Fig. 3, we show the total energy savings versus the number of IoT devices in the case with $K = 3$ UAVs. The total energy savings, as defined in (8a), is the sum of the energy savings experienced by the associated IoT devices when adopting their respective minimum transmit powers, and is measured in millijoules (mJ) in our experiments. The proposed MES device association algorithm is first compared with the case where devices are randomly chosen and associated with their closest UAVs (labeled as "Random" in the figure). The results are first shown under a baseline UAV deployment algorithm where the UAVs' trajectory centers are deployed at the centroid of the K-means clusters of the local devices (labeled as "K-means"). Both the altitude and the radius are set as 150 meters in this case. These values are chosen to ensure that a competitive performance can be achieved by K-means in most cases. Then, the proposed ILB algorithm is applied to further improve the performance. We can see that, under random device association, the total energy savings remains relatively static over the number of devices since the devices' power consumption and demands were not taken into consideration in the association. That is, random sampling does not leverage the benefits of multiuser diversity. On the other hand, the total energy savings of the MES algorithm increases significantly with the

Authorized licensed use limited to: National Tsing Hua Univ.. Downloaded on March 09,2022 at 07:46:55 UTC from IEEE Xplore. Restrictions apply.

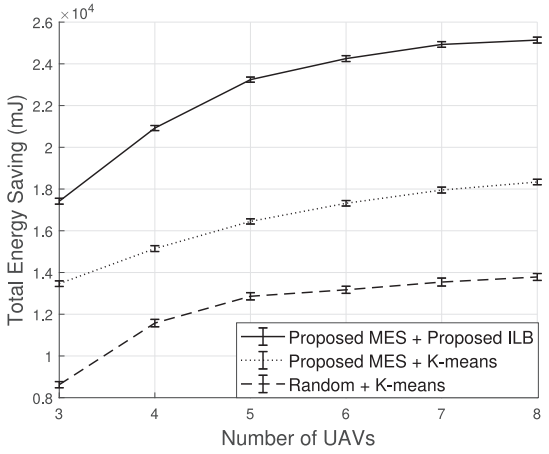

Fig. 4. Total energy savings versus number of UAVs.

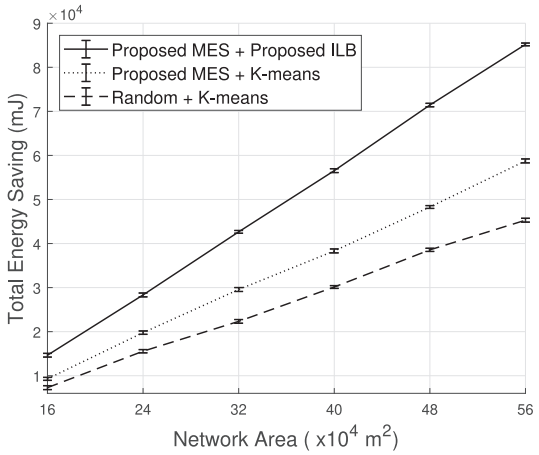

Fig. 5. Total energy savings versus network area for fixed device and UAV densities.

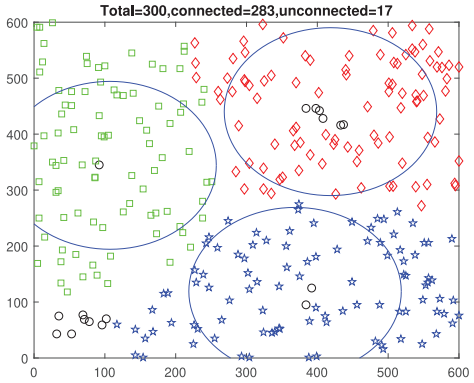

(a) $M = 300$

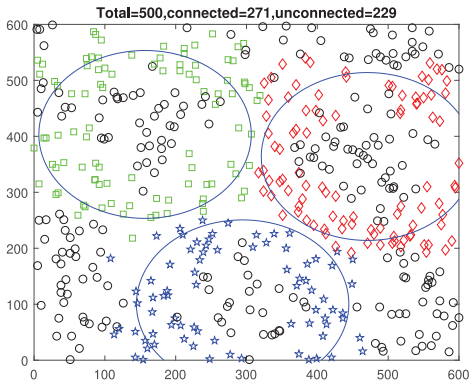

(b) $M = 500$

Fig. 6. Example of resulting device association and UAV deployment. Circle markers represent unassociated devices.

number of devices since the number of devices that can be associated with the UAVs and the multiuser diversity gains that can be exploited by selecting users with large potential energy savings are both increased. However, the gain gradually saturates as the total number of devices increases due to the limited capacities of the UAVs. Moreover, an additional 30% performance gain can be obtained by the adoption of the proposed ILB algorithm. Furthermore, by averaging over 20 realizations, we find that the ILB algorithm (i.e., Algorithm 2) converges rapidly in 10.8, 10.8, and 10.85 iterations for cases with 300, 400, and 500 devices, respectively.

In Fig. 4, we show the total energy savings versus the number of UAVs for a network with $M = 500$ devices. We can see that, as the number of UAVs increases, the energy savings increases in all cases since more devices can be served and their distances to the associated UAVs are decreased. However, the improvement saturates when the number of UAVs is sufficiently large since, in this case, the total capacity of the UAV is enough to serve all devices. Moreover, in Fig. 5, we show the total energy savings versus the network area with fixed device and UAV densities. In particular, the network area in the x-axis increases linearly (taking on the values 16×10^4, 24×10^4, 32×10^4, 40×10^4, 48×10^4, and 56×10^4 m^2) whereas the densities of the devices and the UAVs are fixed as 100 devices and 1 UAV per 100 m^2. That is, the ratio between the number of devices and the number of UAVs is fixed as 100. We can see that the total energy savings increases linearly with the network area since the number of UAVs and the number of devices that can be served by the UAVs scale linearly with the network area as well.

In Fig. 6, we show an example of the device association for cases where the number of UAVs is $K = 3$ and the number of devices is $M = 300$ and 500, respectively. We can see that the number of unassociated devices (i.e., black circle markers) increases as M increases. Notice that the unassociated devices may be located close to the trajectory centers since they are farther away from the circulating UAVs. This is contrary to rotary-wing UAVs that do not need to follow a circle trajectory, but can stay at a static position at the center.

In Fig. 7, we compare the total energy savings attainable by the MES device association algorithm with ideal scheduling, the MES association algorithm with conflict-free scheduling (as proposed in Section VI-A), and the greedy conflict-aware association algorithm. The ideal MES association algorithm refers to the ideal case where all devices are allowed to transmit regardless of any possible collision, whereas the greedy conflict-aware association algorithm selects only devices whose ideal transmission durations are non-overlapping in decreasing order of their normalized demand λ_m/μ_k. Fig. 7(a) shows the total energy savings versus the number of devices for a network with $K = 3$ UAVs. We can see that, as the number of devices increases, the gap between the MES association with ideal scheduling and the greedy conflict-aware association algorithm increases

Authorized licensed use limited to: National Tsing Hua Univ.. Downloaded on March 09,2022 at 07:46:55 UTC from IEEE Xplore. Restrictions apply.

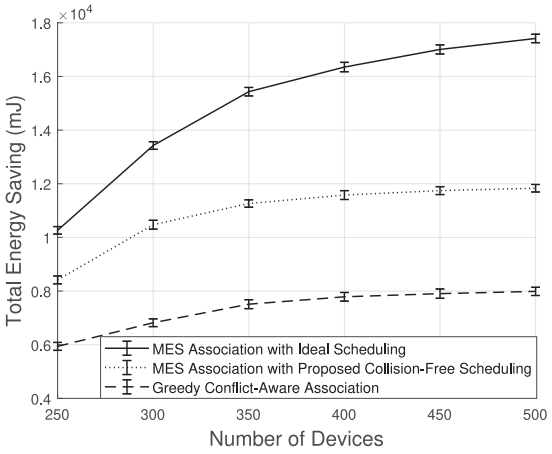

(a) Total energy savings versus number of devices.

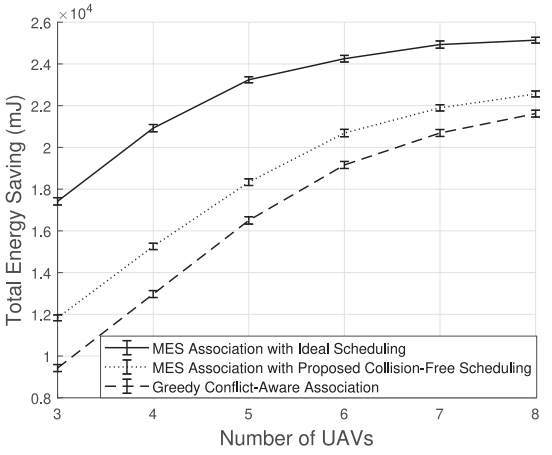

(b) Total energy savings versus number of UAVs.

Fig. 7. Comparison of the total energy savings attainable by the ideal MES association algorithm, the ideal MES with collision-free scheduling, and the greedy conflict-aware association.

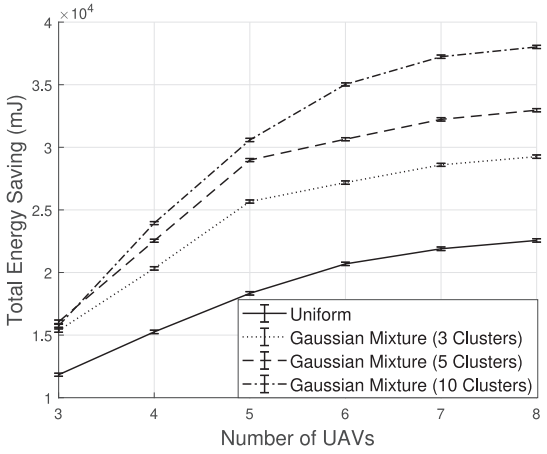

Fig. 8. Total energy savings versus the number of UAVs under the uniform and Gaussian mixture device distributions.

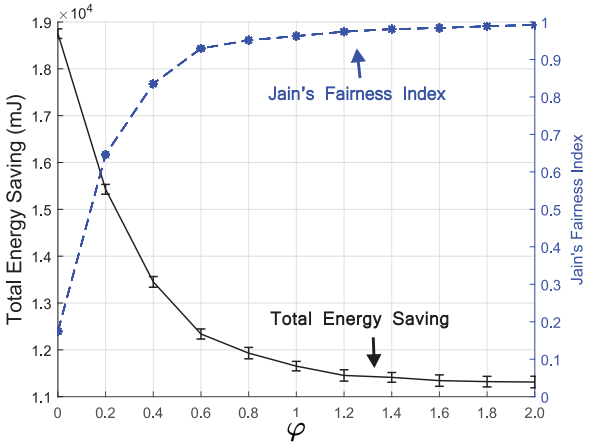

Fig. 9. Total energy savings (black curve) and Jain's fairness index (blue curve) with respect to the freshness parameter φ.

since more conflict may occur under ideal scheduling. With the proposed collision-free scheduling, all devices associated under the MES algorithm are allowed to transmit and, thus, the total energy savings (obtained under ideal scheduling) is better preserved compared to the greedy association algorithm. However, the loss in total energy savings still increases as the number of devices increases since the offset in the devices actual transmission phases will become larger. Moreover, Fig. 7(b) shows the total energy savings versus the number of UAVs for a network with $M = 500$ devices. In this case, the gap between the total energy savings achievable by the ideal and the collision-free scheduling (as well as the greedy conflict-aware association) decreases as the number of UAVs increases since the traffic load of each UAV is decreased and, thus, there will be less overlap between the ideal transmission durations of different devices.

In Fig. 8, we show the impact of the spatial distribution of the devices on the total energy savings achievable under the proposed algorithm. More specifically, we assume that the devices' locations follow a Gaussian mixture distribution with 3, 5, and 10 clusters, respectively. The mean of the different clusters are chosen randomly according to a uniform distribution in a [50, 550] $\times$ [50, 550] m^2 area, and the variance is equal to 300 for both dimensions in all clusters. All clusters have equal prior probabilities. We can see that, with a smaller number of clusters, the devices are more concentrated at certain locations and, thus, their transmission durations will have more overlap, causing the total energy savings to be reduced significantly under the proposed collision-free scheduling. However, as the number of clusters increase, the devices are less concentrated, allowing the total energy savings to increase.

In Fig. 9, we show the effectiveness of the proposed fair device association algorithm with data-freshness weighting. Here, we plot both the total energy savings and Jain's fairness index with respect to the freshness parameter $\varphi_m = \varphi$, for all m. The number of UAVs is $K = 3$ and the number of devices is $M = 800$. Following the definition in [45], we define Jain's fairness index as

$$J\left(\bar{T}_1, \bar{T}_2, \ldots, \bar{T}_M\right) \triangleq \frac{\left(\frac{1}{n}\sum_{m=1}^{M} \bar{T}_m\right)^2}{\frac{1}{n}\sum_{m=1}^{M} \bar{T}_m^2},$$

where $\bar{T}_m$ is defined as the average value of T_m before the data is updated by device m. That is, we use the variation of the average outdatedness of the devices as a measure of fairness. Recall that the outdatedness T_m is initiated by the value of a flight cycle T and is incremented by T whenever device m fails to associate with any UAV within a cycle. Notice

Authorized licensed use limited to: National Tsing Hua Univ.. Downloaded on March 09,2022 at 07:46:55 UTC from IEEE Xplore. Restrictions apply.

that Jain's fairness index (i.e., $J(\bar{T}_1, \bar{T}_2, \ldots, \bar{T}_M)$) must take on a value within the interval $[\frac{1}{M}, 1]$. A larger value implies that the devices are served more fairly and a smaller value implies otherwise. In fact, the largest value 1 is achieved when $\bar{T}_1 = \bar{T}_2 = \cdots = \bar{T}_M$. In this experiment, we fix the UAVs' locations as the position obtained by iterating between the original MES plus ILB algorithms, and utilize the data-freshness weighted objective in (29) only to update the device association in each flight cycle. We can see that, as φ increases, more weighting is given on the importance of data freshness. Hence, devices that have not transmitted for some time are given higher priorities to transmit and, thus, Jain's fairness index increases. However, the improved fairness comes at the cost of reduced total energy savings since the device with larger energy savings may no longer be associated in each cycle.

VIII. Conclusion

In this work, we proposed a joint UAV deployment and device association policy that aims to maximize the total energy savings of the IoT devices during the data-gathering process. Different from most works in the literature, we considered fixed-wing UAVs that must maintain constant movement in order to stay afloat and, thus, follow circular flight trajectories to periodically gather data from their associated devices. Given the UAVs' trajectory centers and flight radii, we first proposed the MES device association algorithm based on an approximation of the 0-1 multiple knapsack problem. Then, given the device association, we further proposed the ILB UAV deployment and flight radius adjustment algorithm that takes into consideration the devices' demands in their iterative updates. Furthermore, to resolve collision among close-by devices and to ensure fairness, we further proposed a collision-free scheduling policy based on the minimization of the transmission phase offset and a modified device association algorithm that balances the freshness of data received from multiple devices at their respective UAVs. Computer simulations showed that, for $K = 3$ and $M = 500$, the proposed MES device association with ILB UAV placement yields almost 100% improvement in terms of the total energy savings compared to the random association and K-means UAV placement, and 30% improvement compared to only MES association. The collision-free scheduling was also shown to effectively preserve the achievable energy savings compared to the greedy conflict-aware association where devices are simply dropped if a collision may occur.

References

[1] M. Mozaffari, W. Saad, M. Bennis, Y.-H. Nam, and M. Debbah, "A tutorial on UAVs for wireless networks: Applications, challenges, and open problems," *IEEE Commun. Surveys Tuts.*, vol. 21, no. 3, pp. 2334–2360, 3rd Quart., 2019.

[2] Y. Zeng, R. Zhang, and T. J. Lim, "Wireless communications with unmanned aerial vehicles: Opportunities and challenges," *IEEE Commun. Mag.*, vol. 54, no. 5, pp. 36–42, May 2016.

[3] M. Erdelj, E. Natalizio, K. R. Chowdhury, and I. F. Akyildiz, "Help from the sky: Leveraging UAVs for disaster management," *IEEE Pervasive Comput.*, vol. 16, no. 1, pp. 24–32, Jan.–Mar. 2017.

[4] F. Cheng *et al.*, "UAV trajectory optimization for data offloading at the edge of multiple cells," *IEEE Trans. Veh. Technol.*, vol. 67, no. 7, pp. 6732–6736, Jul. 2018.

[5] P. Zhan, K. Yu, and A. L. Swindlehurst, "Wireless relay communications with unmanned aerial vehicles: Performance and optimization," *IEEE Trans. Aerosp. Electron. Syst.*, vol. 47, no. 3, pp. 2068–2085, Jul. 2011.

[6] Y. Zeng, R. Zhang, and T. J. Lim, "Throughput maximization for UAV-enabled mobile relaying systems," *IEEE Trans. Commun.*, vol. 64, no. 12, pp. 4983–4996, Dec. 2016.

[7] J. Wang, C. Jiang, Z. Han, Y. Ren, R. G. Maunder, and L. Hanzo, "Taking drones to the next level: Cooperative distributed unmanned-aerial-vehicular networks for small and mini drones," *IEEE Veh. Technol. Mag.*, vol. 12, no. 3, pp. 73–82, Jul. 2017.

[8] N. H. Motlagh, M. Bagaa, and T. Taleb, "UAV-based IoT platform: A crowd surveillance use case," *IEEE Commun. Mag.*, vol. 55, no. 2, pp. 128–134, Feb. 2017.

[9] N. H. Motlagh, T. Taleb, and O. Arouk, "Low-altitude unmanned aerial vehicles-based Internet of Things services: Comprehensive survey and future perspectives," *IEEE Internet Things J.*, vol. 3, no. 6, pp. 899–922, Dec. 2016.

[10] C. Zhan, Y. Zeng, and R. Zhang, "Energy-efficient data collection in UAV enabled wireless sensor network," *IEEE Wireless Commun. Lett.*, vol. 7, no. 3, pp. 328–331, Jun. 2018.

[11] J. Gong, T. Chang, C. Shen, and X. Chen, "Flight time minimization of UAV for data collection over wireless sensor networks," *IEEE J. Sel. Areas Commun.*, vol. 36, no. 9, pp. 1942–1954, Sep. 2018.

[12] M. Mozaffari, W. Saad, M. Bennis, and M. Debbah, "Mobile unmanned aerial vehicles (UAVs) for energy-efficient Internet of Things communications," *IEEE Trans. Wireless Commun.*, vol. 16, no. 11, pp. 7574–7589, Nov. 2017.

[13] M. Mozaffari, W. Saad, M. Bennis, and M. Debbah, "Wireless communication using unmanned aerial vehicles (UAVs): Optimal transport theory for hover time optimization," *IEEE Trans. Wireless Commun.*, vol. 16, no. 12, pp. 8052–8066, Dec. 2017.

[14] K.-M. Chen, T.-H. Chang, and T.-S. Lee, "Lifetime maximization for uplink transmission in UAV-enabled wireless networks," in *Proc. IEEE Int. Conf. Wireless Commun. Netw. Conf. (WCNC)*, 2019, pp. 1–6.

[15] J. Wang, C. Jiang, Z. Wei, C. Pan, H. Zhang, and Y. Ren, "Joint UAV hovering altitude and power control for space-air-ground IoT networks," *IEEE Internet Things J.*, vol. 6, no. 2, pp. 1741–1753, Apr. 2019.

[16] Q. Wu, Y. Zeng, and R. Zhang, "Joint trajectory and communication design for multi-UAV enabled wireless networks," *IEEE Trans. Wireless Commun.*, vol. 17, no. 3, pp. 2109–2121, Mar. 2018.

[17] G. Yang, R. Dai, and Y.-C. Liang, "Energy-efficient UAV backscatter communication with joint trajectory design and resource optimization," *IEEE Trans. Wireless Commun.*, vol. 20, no. 2, pp. 926–941, Feb. 2021.

[18] Y.-W. P. Hong, R.-H. Cheng, Y.-C. Hsiao, and J.-P. Sheu, "Power-efficient trajectory adjustment and temporal routing for multi-UAV networks," *IEEE Trans. Green Commun. Netw.*, vol. 4, no. 4, pp. 1106–1119, Dec. 2020.

[19] M. Dawande, J. Kalagnanam, P. Keskinocak, F. S. Salman, and R. Ravi, "Approximation algorithms for the multiple knapsack problem with assignment restrictions," *J. Comb. Optim.*, vol. 4, no. 2, pp. 171–186, 2000.

[20] S. Martello, *Knapsack Problems: Algorithms and Computer Implementations* (Wiley-Interscience Series in Discrete Mathematics and Optimization). New York, NY, USA: Wiley, 1990.

[21] A. Al-Hourani, S. Kandeepan, and S. Lardner, "Optimal LAP altitude for maximum coverage," *IEEE Wireless Commun. Lett.*, vol. 3, no. 6, pp. 569–572, Dec. 2014.

[22] R. I. Bor-Yaliniz, A. El-Keyi, and H. Yanikomeroglu, "Efficient 3-D placement of an aerial base station in next generation cellular networks," in *Proc. IEEE Int. Conf. Commun. (ICC)*, 2016, pp. 1–5.

[23] Y. Zeng and R. Zhang, "Energy-efficient UAV communication with trajectory optimization," *IEEE Trans. Wireless Commun.*, vol. 16, no. 6, pp. 3747–3760, Jun. 2017.

[24] Y. Zeng, J. Xu, and R. Zhang, "Energy minimization for wireless communication with rotary-wing UAV," *IEEE Trans. Wireless Commun.*, vol. 18, no. 4, pp. 2329–2345, Apr. 2019.

[25] M. Mozaffari, W. Saad, M. Bennis, and M. Debbah, "Unmanned aerial vehicle with underlaid device-to-device communications: Performance and tradeoffs," *IEEE Trans. Wireless Commun.*, vol. 15, no. 6, pp. 3949–3963, Jun. 2016.

[26] J. Gu, H. Wang, G. Ding, Y. Xu, Z. Xue, and H. Zhou, "Energy-constrained completion time minimization in UAV-enabled Internet of Things," *IEEE Internet Things J.*, vol. 7, no. 6, pp. 5491–5503, Jun. 2020.

[27] H. Wang, J. Wang, G. Ding, L. Wang, T. A. Tsiftsis, and P. K. Sharma, "Resource allocation for energy harvesting-powered D2D communication underlaying UAV-assisted networks," *IEEE Trans. Green Commun. Netw.*, vol. 2, no. 1, pp. 14–24, Mar. 2018.

Authorized licensed use limited to: National Tsing Hua Univ.. Downloaded on March 09,2022 at 07:46:55 UTC from IEEE Xplore. Restrictions apply.

[28] M. Hua, Y. Wang, Z. Zhang, C. Li, Y. Huang, and L. Yang, "Power-efficient communication in UAV-aided wireless sensor networks," *IEEE Commun. Lett.*, vol. 22, no. 6, pp. 1264–1267, Jun. 2018.
[29] C. Zhan, Y. Zeng, and R. Zhang, "Trajectory design for distributed estimation in UAV-enabled wireless sensor network," *IEEE Trans. Veh. Technol.*, vol. 67, no. 10, pp. 10155–10159, Oct. 2018.
[30] S. Yeh, Y. Wang, T. D. P. Perera, Y.-W. P. Hong, and D. N. K. Jayakody, "UAV trajectory optimization for data-gathering from backscattering sensor networks," in *Proc. IEEE Int. Conf. Commun. (ICC)*, 2020, pp. 1–6.
[31] S. Say, H. Inata, J. Liu, and S. Shimamoto, "Priority-based data gathering framework in UAV-assisted wireless sensor networks," *IEEE Sensors J.*, vol. 16, no. 14, pp. 5785–5794, Jul. 2016.
[32] H. El Hammouti, M. Benjillali, B. Shihada, and M.-S. Alouini, "A distributed mechanism for joint 3D placement and user association in UAV-assisted networks," in *Proc. IEEE Wireless Commun. Netw. Conf.*, 2019, pp. 1–6.
[33] J. Wang *et al.*, "Multiple unmanned-aerial-vehicles deployment and user pairing for nonorthogonal multiple access schemes," *IEEE Internet Things J.*, vol. 8, no. 3, pp. 1883–1895, Feb. 2021.
[34] E. Koyuncu, M. Shabanighazikelayeh, and H. Seferoglu, "Deployment and trajectory optimization of UAVs: A quantization theory approach," *IEEE Trans. Wireless Commun.*, vol. 17, no. 12, pp. 8531–8546, Dec. 2018.
[35] X. Zhang and L. Duan, "Fast deployment of UAV networks for optimal wireless coverage," *IEEE Trans. Mobile Comput.*, vol. 18, no. 3, pp. 588–601, Mar. 2019.
[36] C. Shen, T.-H. Chang, J. Gong, Y. Zeng, and R. Zhang, "Multi-UAV interference coordination via joint trajectory and power control," *IEEE Trans. Signal Process.*, vol. 68, pp. 843–858, 2020.
[37] X. Li, H. Yao, J. Wang, X. Xu, C. Jiang, and L. Hanzo, "A near-optimal UAV-aided radio coverage strategy for dense urban areas," *IEEE Trans. Veh. Technol.*, vol. 68, no. 9, pp. 9098–9109, Sep. 2019.
[38] C. Zhan and Y. Zeng, "Completion time minimization for multi-UAV-enabled data collection," *IEEE Trans. Wireless Commun.*, vol. 18, no. 10, pp. 4859–4872, Oct. 2019.
[39] N. Wang *et al.*, "Priority-oriented trajectory planning for UAV-aided time-sensitive IoT networks," in *Proc. IEEE Int. Conf. Commun. Workshops (ICC Workshops)*, 2020, pp. 1–7.
[40] C. Luo, M. N. Satpute, D. Li, Y. Wang, W. Chen, and W. Wu, "Fine-grained trajectory optimization of multiple UAVs for efficient data gathering from WSNs," *IEEE/ACM Trans. Netw.*, vol. 29, no. 1, pp. 162–175, Feb. 2021.
[41] H. J. Na and S. Yoo, "PSO-based dynamic UAV positioning algorithm for sensing information acquisition in wireless sensor networks," *IEEE Access*, vol. 7, pp. 77499–77513, 2019.
[42] T. H. Cormen, C. E. Leiserson, R. L. Rivest, and C. Stein, *Introduction to Algorithms*. Cambridge, MA, USA: MIT Press, 2009.
[43] S. Boyd, S. P. Boyd, and L. Vandenberghe, *Convex Optimization*. Cambridge, U.K.: Cambridge Univ. Press, 2004.
[44] M. Bouzeghoub, "A framework for analysis of data freshness," in *Proc. Int. Workshop Inf. Qual. Inf. Syst. (IQIS)*, 2004, pp. 59–67.
[45] R. Jain, D. Chiu, and W. Hawe, "A quantitative measure of fairness and discrimination for resource allocation in shared computer systems," DEC, Maynard, MA, USA, Res. Rep. TR-301, 1984.

Yung-Ching Kuo (Graduate Student Member, IEEE) received the B.S. degree in information management from Tunghai University, Taiwan, in 2015, and the master's degree from National Tsing Hua University, where he is currently pursuing the Doctoral degree with the Department of Computer Science. His research interests include wireless communications, mobile computing, Internet of Things, and UAV networking. He was awarded the Principal's Scholarship from National Tsing Hua University, due to his outstanding academic performance.

Jen-Hao Chiu received the B.S. degree in computer science from National Central University, Taoyuan, Taiwan, in 2017, and the M.S. degree in computer science from National Tsing Hua University, Hsinchu, Taiwan, in 2019. His research interests include UAV communications, power control, resource allocation, and Internet of Things.

Jang-Ping Sheu (Fellow, IEEE) received the B.S. degree in computer science from Tamkang University, Taiwan, in 1981, and the M.S. and Ph.D. degrees in computer science from National Tsing Hua University, Taiwan, in 1983 and 1987, respectively. He is currently a Chair Professor of the Department of Computer Science and the Director of the Joint Research Center of Delta-NTHU, National Tsing Hua University, where he was an Associate Dean of the College of Electrical and Computer Science from 2016 to 2017, and the Director of the Computer and Communication Research Center from 2009 to 2015. He was a Director of Computer Center, National Central University from 2003 to 2006, where he was a Director of the Department of Computer Science and Information Engineering from 1997 to 1999. His current research interests include wireless communications, mobile computing, Internet of Things, and UAV-assisted communication systems. He received the Distinguished Research Awards of the National Science Council of the Republic of China from 1993 to 1994, from 1995 to 1996, and from 1997 to 1998, the Distinguished Engineering Professor Award of the Chinese Institute of Engineers in 2003, the K. -T. Li Research Breakthrough Award of the Institute of Information and Computing Machinery (IICM) in 2007, and the Y. Z. Hsu Scientific Chair Professor Award and the Pan Wen Yuan Outstanding Research Award in 2009 and 2014, respectively, the Academic Award in Engineering from the Ministry of Education in 2016, the Medal of Honor in Information Sciences from the IICM in 2017, and the TECO Award in 2019. He was an Associate Editor of the IEEE TRANSACTIONS ON PARALLEL AND DISTRIBUTED SYSTEMS and the INTERNATIONAL JOURNAL OF SENSOR NETWORKS. He is an Advisory Board Member of the *International Journal of Ad Hoc and Ubiquitous Computing* and *International Journal of Vehicle Information and Communication Systems*. He is a member of the Phi Tau Phi Society.

Y.-W. Peter Hong (Senior Member, IEEE) received the B.S. degree in electrical engineering from National Taiwan University, Taipei, Taiwan, in 1999, and the Ph.D. degree in electrical engineering from Cornell University, Ithaca, NY, USA, in 2005.

He joined the Institute of Communications Engineering and the Department of Electrical Engineering with National Tsing Hua University (NTHU), Hsinchu, Taiwan, in 2005, where he is currently a Full Professor. He also serves as Associate Vice President of Research and Development, NTHU. His research interests include multiuser communications, physical layer security, machine learning for wireless communications, and distributed signal processing for IoT and sensor networks. He received the IEEE ComSoc Asia–Pacific Outstanding Young Researcher Award in 2010, the Y. Z. Hsu Scientific Paper Award in 2011, the National Science Council Wu Ta-You Memorial Award in 2011, the Chinese Institute of Electrical Engineering Outstanding Young Electrical Engineer Award in 2012, the Best Paper Award from the Asia–Pacific Signal and Information Processing Association Annual Summit and Conference in 2013, and the Ministry of Science and Technology Outstanding Research Award in 2019. He is currently serves as Senior Area Editor of IEEE TRANSACTIONS ON SIGNAL PROCESSING. Previously, he also served on the editorial boards of IEEE TRANSACTIONS ON SIGNAL PROCESSING, IEEE TRANSACTIONS ON INFORMATION FORENSICS AND SECURITY, and IEEE TRANSACTIONS ON COMMUNICATIONS. He is currently a Vice Chair of IEEE Taipei Section, and a Secretary of IEEE ComSoc Communication Theory Technical Committee. In the past, he also served as a Chair of the IEEE ComSoc Taipei Chapter from 2017 to 2018, and a Co-Chair of the Technical Affairs Committee, the Information Services Committee, and the Chapter Coordination Committee of the IEEE ComSoc Asia–Pacific Board from 2014 to 2015, from 2016 to 2019, and from 2020 ton 2021, respectively.

Authorized licensed use limited to: National Tsing Hua Univ.. Downloaded on March 09,2022 at 07:46:55 UTC from IEEE Xplore. Restrictions apply.